Journal of Plant Growth Regulation (2025) 44:1753–1766
https://doi.org/10.1007/s00344-024-11453-1

Uncovering miRNA-Mediated Regulation in Phellem Versus Xylem Differentiation in *Quercus suber* L.

Susana T. Lopes[1,2,3] · Bruno Costa[1,3] · Inês Chaves[1,2,3] · Augusta Costa[4] · Célia M. Miguel[1,3]

Received: 23 June 2023 / Accepted: 2 August 2024 / Published online: 22 August 2024

Abstract

Several regulators of phellem/cork formation have been identified in recent years, using mainly transcriptomic approaches. However, this developmental process, showing parallels to the functioning of vascular cambium, remains poorly understood. The cork oak tree (*Quercus suber* L.) exhibits a remarkable ability to form a traumatic phellogen after debarking, enabling sustainable cork production. We aimed at uncovering post-transcriptional mechanisms controlled by miRNAs, specifically involved in regulating phellogen functioning and phellem differentiation in cork oak. To achieve this, we conducted a comparative analysis of the small RNA transcriptome between differentiating phellem and xylem, both originating from secondary meristems (phellogen and vascular cambium). In addition to identifying miRNAs exclusive to phellogen/phellem tissues, we discovered 246 differentially expressed miRNAs between the two tissues, of which 74 are conserved. The most abundant miRNA families found in phellem tissues were MIR165/166, MIR167, MIR168 and MIR390. By analysing miRNA predicted targets and their expression in the same tissues, many of the differentially expressed miRNAs were found associated with sequence-specific DNA binding functions. Within these, transcription factor families HD-ZIP III, WRKY, NAC and MYB were highlighted as key in phellem differentiation. Furthermore, hormone-mediated signalling pathways, particularly involving auxin, appeared as an enriched biological process, as several ARF transcripts, among other auxin signalling genes like IAA11, ARF18 and ARF19, were identified as putative targets of conserved or novel miRNAs. Overall, our results provide a comprehensive overview of the miRNA landscape during cork formation, providing valuable knowledge for further functional studies and potential practical applications in forest management.

Handling Editor: Vinay Kumar.

✉ Célia M. Miguel
cmmiguel@fc.ul.pt

[1] Instituto de Biologia Experimental e Tecnológica (iBET), Oeiras, Portugal

[2] Instituto de Tecnologia Química e Biológica António Xavier, Universidade Nova de Lisboa (ITQB NOVA), Oeiras, Portugal

[3] Biosystems and Integrative Sciences Institute, Faculdade de Ciências, Universidade de Lisboa (FCUL), Lisbon, Portugal

[4] Instituto Nacional de Investigação Agrária e Veterinária (INIAV), Oeiras, Portugal

Graphical Abstract

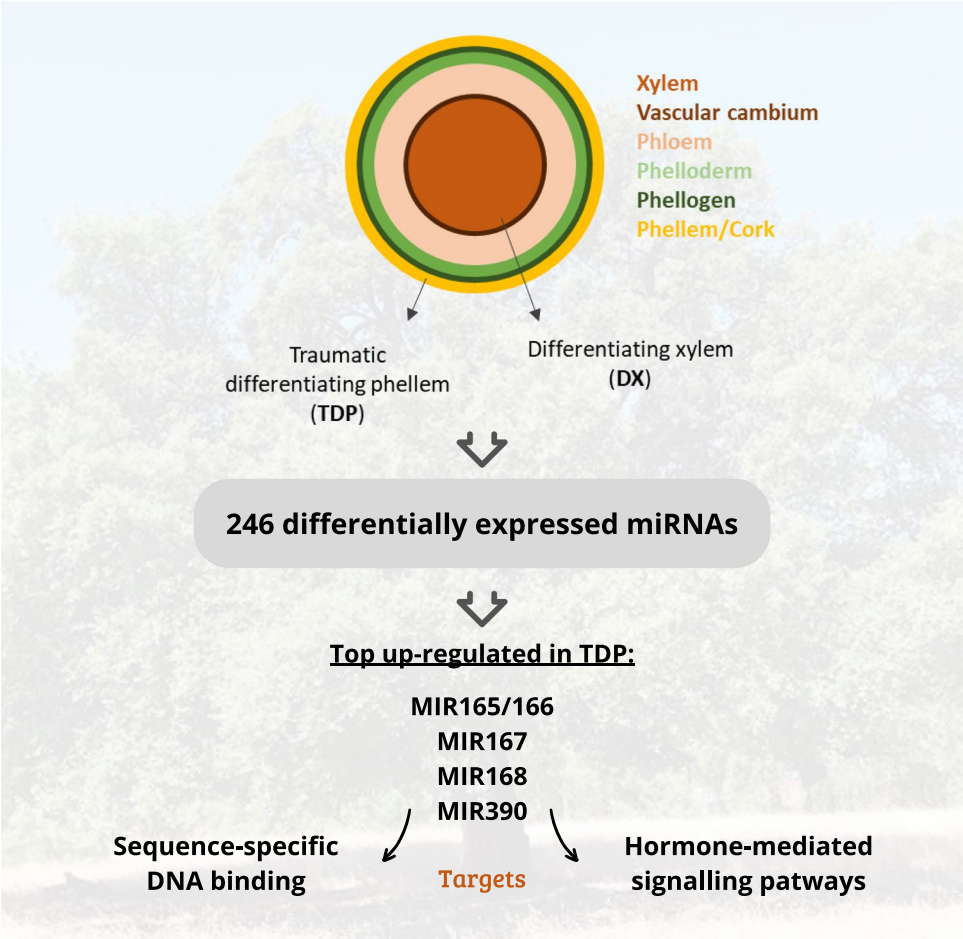

Keywords Cork oak · Secondary growth · Phellogen/phellem · MicroRNAs

Introduction

Small non-coding RNAs (sRNAs) are involved in the regulation of gene expression in eukaryotic and prokaryotic organisms, and even in viruses. In plants, sRNAs can broadly be classified as small interfering RNAs (siRNAs), when they derive from a double-stranded RNA precursor or as hairpin RNAs if their precursor is a single-stranded RNA. The latter include the microRNAs (miRNAs) (Axtell 2013), which are one of the best-studied sRNA classes. MiRNAs, typically 20–22 nucleotides (nt) long, are highly complementary to their mRNA targets, usually presenting less than 4 mismatches (Jones-Rhoades 2012; Li et al. 2017a, b), and mediate post-transcriptional gene silencing via transcript cleavage or translation inhibition (Axtell 2013; Borges and Martienssen 2015; Li et al. 2017a, b). While conserved miRNAs, which are present in multiple plant species with homologous target mRNA, may show high expression levels, novel miRNAs or lineage-specific miRNAs have been typically reported as low abundant, expressed in specific tissues, and sometimes lacking functional targets as a result of their transient nature (Jones-Rhoades 2012; Axtell 2013; Qin et al. 2014).

Many miRNAs are key regulators of several biological processes, including plant growth and development, hormone signalling, maintenance of homeostasis and response to biotic and abiotic stresses. Meristem-related functions have also been associated to miRNA roles, both in primary meristems (Laufs et al. 2004; Williams et al. 2005; Zhang and Zhang 2012; Knauer et al. 2013; Chang et al. 2020; Wang et al. 2021) and during secondary growth (Lopes et al. 2020). Secondary growth leads to a girth increase of stems and older branches and roots, brought about by the functioning of two secondary meristems: the vascular cambium, responsible for generating xylem inwards and phloem outwards, and the cork cambium (or phellogen), which gives

rise to the phelloderm internally and phellem (also known as cork) externally, resulting in the formation of the periderm. While all the secondary tissues formed are important for the overall structure and function of the plant, the phellem (or cork) and the secondary xylem (or wood) of different species are of high value for forest industries worldwide, having multiple applications in construction, paper and pulp, furniture, wine stoppers, among others. Therefore, several studies have been conducted in this subject, especially focusing on the vascular development.

MiRNA165/166 has been implicated in several aspects of secondary growth from the vascular cambium by targeting CLASS III HOMEODOMAIN-LEUCINE ZIPPER (HD-ZIP III) members, which are involved in cambium initiation and patterning of secondary vascular tissues (Emery et al. 2003; Mallory et al. 2004; Ko et al. 2006; Zhou et al. 2007; Ilegems et al. 2010; Robischon et al. 2011). The regulation of class III HD-ZIPs by miRNA165/166 also seems to be involved in the control of seasonal cessation of growth or dormancy release in trees (Ko et al. 2006; Barakat et al. 2007). Other miRNAs, including miR164, miR162, miR168, miR395 and miR396, have shown specific roles in vascular development (Tang et al. 2016; Liu et al. 2022; Wang et al. 2022) or a dominant expression in the secondary vascular development zone in *Populus* (Dharmawardhana et al. 2010). Furthermore, high-throughput sequencing approaches revealed several xylem-enriched miRNA targets involved in secondary growth, such as genes coding for vascular-related transcription factors and enzymes associated with reaction wood formation (Puzey et al. 2012).

While some progress has been made in understanding the regulation of vascular development from the cambium by miRNAs, far less is known about the post-transcriptional regulation of phellogen activity and periderm development. A single report by Chaves et al. (2014) has described the expression patterns of miRNAs in differentiating phellem when compared to leaf tissues of *Quercus suber* L. This study allowed the identification of 41 families of conserved miRNAs and 30 novel miRNAs, from which 13 were uniquely present in phellem. Whereas the conserved miRNA families MIR159, MIR165/166, MIR167 and MIR396 were the most highly expressed in both leaf and phellem, miR168 and miR390 were more represented in phellem. Phellem-specific miRNA families were also identified (MIR1140, MIR158, MIR1863, MIR2916, MIR479, MIR5083 and MIR530) (Chaves et al. 2014). Some of these miRNAs have previously been associated with vascular development and secondary growth.

Although parallels in regulatory pathways between different meristems have been highlighted (Soler et al. 2008; Ragni and Greb 2018), uncovering the expression networks and miRNA-specific involvement in phellogen functioning and phellem differentiation would be of great interest. *Q. suber*, commonly known as cork oak, is an evergreen tree species that exhibits remarkable ability in phellogen self-regeneration and cork differentiation, being mostly found across the Mediterranean region in agro-silvo-pastoral ecosystems called "montado" in Portugal, or "dehesa" in Spain, with key economic, social and environmental roles. Cork is a renewable material with valuable applications due to properties such as low density, low permeability, and elasticity, providing high insulation and damping capacities (Pereira 2007), and therefore representing a valuable raw material for a highly profitable industry in the regions where it is produced. The cork oak tree undergoes its first harvest when it reaches around 18–25 years of age, yielding a poor-quality cork, known as "virgin" cork. After the cork stripping process, meristematic activity increases, leading to the formation of a traumatic phellogen, which generates a new layer of cork. Subsequent cork stripping is performed every 9 years and, starting from the third harvest, the cork exhibits improved quality traits and higher economic value, known as "amadia" or reproduction cork (Natividade 1950; Graça and Pereira 2004).

In a previous study, a genome-wide transcriptomics approach was employed to compare the expression profiles of coding transcripts in xylem and phellogen/phellem tissues of *Q. suber*. This analysis revealed regulatory pathways putatively unique to phellogen activity and phellem differentiation (Lopes et al. 2020). A shortlist of promising candidate genes, including novel genes involved in the suberization process, as well as genes associated with ethylene and jasmonate signalling and meristem function, was identified as important for the formation and differentiation of phellogen/phellem (Lopes et al. 2020). Given the relevance of the cork formation process both from biological and biotechnological perspectives, in the present study we aimed at the identification of specific miRNAs and their putatively associated functions specifically involved in this process. By comparing the expression profiles of phellem and xylem tissues, we were able to filter out miRNA candidates overall involved in secondary growth and instead focus on miRNAs putatively involved in phellogen activity and cork differentiation in cork oak trees. Furthermore, we compared "virgin" and "amadia" cork to investigate the molecular processes that contribute to the distinct characteristics of each type of phellem tissue.

The first comprehensive overview of the miRNA landscape in phellogen and differentiating phellem of cork oak trees is here provided, representing a valuable basis for further functional studies and potential applications in forest management.

Materials and Methods

Sampling and RNA Preparation

Harvesting procedures and plant material used in this study are the same as those described in Lopes et al. (2020). All the samples were collected during the active growth period from adult cork oak trees showing extensive secondary growth, i.e. phellem and secondary xylem formation from the phellogen and vascular cambium, respectively. For each type of tissue samples (phellem or xylem), harvested trees were growing in the same area and therefore subject to the same environmental conditions. A total of six adult trees were sampled from a cork oak stand (*montado*) in Benavente (Companhia das Lezírias, Portugal—38° 52′ 44.3″ N 8° 51′ 43.2″ W), to collect "amadia" and "virgin" cork samples (phellogen/phellem) by scrapping the inner side of cork planks immediately after their removal, during the cork harvesting season, which corresponds to the active growth period. To simplify, hereafter, we will refer to these samples as phellem although they contain both phellem and phellogen cells. According to the nomenclature defined in Lopes et al. (2020), samples collected from "amadia" cork planks were named traumatic differentiating phellem (TDP), while samples collected from "virgin" cork planks were named original differentiating phellem (ODP).

Xylem samples were collected from three adult "amadia" trees, in a research dedicated field-station (Centre for Environmental Biology, Universidade de Lisboa), located in Serra de Grândola (Herdade da Ribeira Abaixo, Portugal—38° 06′ 29.1″ N 8° 34′ 08.4″ W), by scrapping the tree stem, after removing a small block of bark until reaching the vascular cambium, collecting mostly differentiating xylem (DX) and some vascular cambium cells, during the active vegetative growth period. Due to the high content of phenols in cork samples, total RNA, including the small fraction, from TDP and ODP tissues was extracted using the protocol described by Chang et al. (1993) and from DX tissue using the Total RNA Purification Kit (Norgen, Biotech Corp., Ontario, Canada), with slight modifications described in Lopes et al. (2020). Remaining traces of genomic DNA were removed by TURBO DNAse treatment (ThermoFisher Scientific, Massachusetts, USA) and RNA integrity was assessed by agarose gel electrophoresis with Red Safe (iNtRON Biotechnology, Seoul, Korea) staining. MicroRNA concentrations were determined by Qubit microRNA Assay Kit (ThermoFisher Scientific). Three biological replicates of TDP, ODP and DX samples were sent for library preparation and sequencing of sRNAs, through Illumina HiSeq2500 technology (Fasteris, SA).

Small RNA Identification and Differential Expression Analysis

Raw sequenced libraries were processed using miRPursuit v1.2.0 pipeline (Chaves et al. 2017) https://github.com/forestbiotech-lab/miRPursuit, to identify and annotate conserved and novel sRNA sequences.

After the preprocessing step, where the sequencing quality of raw reads was checked and the adaptors removed, a filtering step was performed retaining only the sequences within the 18–26-nt length range with an abundance higher than 5 reads in at least 2 libraries of the same tissue and excluding low complexity and t/rRNA sequences. A second filtering step was applied, where only the reads that mapped perfectly (0 mismatches) against *Q. suber* reference genome (Ramos et al. 2018) were maintained for subsequent analysis. This data matrix was then normalised against the total number of reads in each library times one million (Counts Per Million or CPM), to allow comparison between different libraries. A principal component analysis (PCA) was performed to all libraries (ODP, TDP and DX) using the normalised data of both conserved and novel miRNAs.

The miRNA data/reads filtered against the reference genome were annotated, firstly by mapping them against the mature miRNAs deposited in miRBase v22 database (Kozomara and Griffiths-Jones 2014) to annotate conserved miRNAs and then the precursors for the filtered reads and tasi-RNAs were predicted using the reference genome. The annotation of conserved miRNAs was performed by the module in the pipeline running miRProf (Stocks et al. 2012), set to a maximum of two mismatches. The next step in the miRPursuit pipeline runs miRCat (Moxon et al. 2008), which analyses the reference genome to predict putative hairpin structures that might arise to identify precursors of the conserved miRNAs and generate a list of presumptive novel miRNAs. The last annotation step executed the TaSi Predictor tool (Chen et al. 2007) to identify tasi-RNAs.

Differential expression analysis was performed on the raw read counts obtained from miRPursuit using the bioconductor package edgeR (Robinson et al. 2009), by applying a filter to the p-value corrected for multiple testing by false discovery rate (FDR) < 0.05 and at least two times log-fold-change (logFC $>= 2$). Heatmaps of conserved, novel and tasi-RNAs from TDP and DX tissues were built using CPM expression values and by applying the function $\log(x)+1$ to help illustrate the differences.

Target Prediction and Enrichment Analysis

MiRNA target prediction was performed using psRNATarget online tool (Dai et al. 2018) against the RefSeq release (GCF_002906115.1_CorkOak1.0_genomic) of predicted transcripts from the reference genome deposited in NCBI

genome (Ramos et al. 2018), which is the same reference genome depicted throughout this work. The list of putative targets was merged with the list of transcripts in the RNA-seq data from the same sampled tissues (Lopes et al. 2020), and only the predicted targets present in both datasets were considered for subsequent analysis. To add an additional filter to the differential expression analysis, a Pearson correlation coefficient between miRNAs and their putative targets was calculated in R, using the normalised expression levels. Only the pairs of miRNA target with a correlation coefficient lower than -0.70 were selected for further analysis.

The identified target transcripts were subjected to a functional enrichment analysis using the command line Galaxy implementation of GOEnrichment (Faria 2017. GOEnrichment. GitHub repository. GitHub. Retrieved from https://github.com/DanFaria/GOEnrichment). Gene ontology (GO) terms were obtained from the CorkOakDB (Arias-Baldrich et al. 2020). A Fisher exact test corrected using the Benjamini–Hochberg method was used to determine the *p*-values.

Reverse Transcription Quantitative PCR (RT-qPCR)

Five conserved miRNAs were selected for expression profile validation mainly based on the interesting functions of their putative targets and their differential expression in phellem versus xylem. Due to their high specificity and reliability, TaqMan probes (TaqMan miRNA Assays, Applied Biosystems) were used, namely miR165_1 (TCGGACCAG GCTTCATTCCCC; Assay ID: 000347), miR167_2 (TGA AGCTGCCAGCATGATCTG; Assay ID: 003037_mat), miR168_1 (TCGCTTGGTGCAGGTCGGGAA; Assay ID: 000351), miR390_1 (AAGCTCAGGAGGGATAGCGCC; Assay ID: 001409) and miR399_1 (TGCCAAAGGAGA GCTGCCCTG; Assay ID: 008429_mat). Absolute quantification of miRNA expression was performed through standard curves by using oligonucleotides identical to the selected miRNAs (Biomers.net). RNA extraction from TDP and DX samples was carried out as previously described. MiRNAs were reverse-transcribed using TaqMan® MicroRNA Reverse Transcription Kit (Applied Biosystems®) and the associated miRNA-specific RT primers provided with TaqManAssay® MicroRNA Assay (Applied Biosystems®), following the manufacturer's instructions. RT-qPCR was performed using the LightCycler 480 (Roche Diagnostics) with 96-well white plates (Roche Diagnostics). Each 20 uL qPCR reaction mixture included 1X TaqMan® Universal PCR Master Mix II, No UNG (Applied Biosystems®), 1X TaqMan® MicroRNA Assay (Applied Biosystems®) and the cDNA previously prepared. Three biological replicates, each with three technical replicates, were used. The mean from each biological sample was used to calculate the statistical significance of miRNA expression level using Student's *t*-test (significance at $p < 0.05$). The correlation coefficient (R^2) between RNA-seq and RT-qPCR was calculated through the mean of the three biological replicates for each tissue (TDP and DX).

Data Accessibility

The sequencing data for sRNA reads were deposited in the European Nucleotide Archive under the study PRJEB57737, with the run accessions ERR109026 (60–68).

Results

The *Q. suber* miRNAs and tasi-RNAs presented in this work were identified and annotated based on the genome sequence of *Q. suber* released in 2018 (Ramos et al. 2018), which had not been previously used for this purpose. The generated data allowed the comparative analysis of miRNA expression in differentiating xylem versus phellem tissues of *Q. suber* and the identification of putative miRNA-mediated post-transcriptional regulatory mechanisms prevalent in differentiating phellem. The same approach was applied to compare differentiating phellem formed from original versus traumatic phellogen to help explain the characteristic features of each type of phellem tissue.

sRNA Sequencing and Annotation

Sequencing of the sRNAs obtained from the 9 libraries of *Q. suber* secondary tissues yielded a total of 485,963,485 reads, with an average of 47 M raw reads for ODP, 50 M for TDP and 65 M for DX (Table S1). After sequence quality check and the filtering steps, approximately 17 M reads remained for ODP, 19 M for TDP and 27 M for DX. Approximately 80% of the reads mapped against *Q. suber* reference genome (Ramos et al. 2018). Among the filtered reads, around 1.53–4.56% represent unique (distinct) sequences, with ODP showing the lowest percentage of unique sequences and DX the highest percentage (Table S1). The percentage of filtered reads and the reads mapped against the reference genome were similar between biological replicates in each tissue.

According to the principal component analysis (PCA) (Fig. S1), performed for all libraries after normalisation of sRNA data, the first component (PC1), responsible for most of the variation (> 85%), shows a clear separation between xylem (DX) and differentiating phellem (ODP and TDP). Furthermore, ODP and TDP are only separated by PC2, responsible for less than 15% of the variation. As for the sRNA size profile generated from FASTA (raw) data, most reads are 24 nt long for all tissues, particularly in DX, followed by 21 nt, mainly present in ODP and TDP (Table S2a). After the filtering steps, the higher percentage of 24 nt reads in DX becomes even more evident, with an

increase from 44 to 64%. In TDP libraries, the 24 nt class remains predominant, while in ODP, the 21 nt size class becomes the most abundant (26%) followed by the 24 nt class (22%) (Table S2a and b).

A total of 18,729 distinct sRNAs with expression in at least 2 libraries of the same tissue were identified, with 1538 (8.2%) being exclusive of TDP, 558 (2.98%) of ODP and 7764 (41.45%) of DX (Fig. 1, Table S3). From these, 550 are conserved miRNAs belonging to 70 different families, 17,656 were annotated as novel miRNAs and 523 as tasi-RNAs (Table S3).

miRNAs Exclusive of Periderm Tissues and Their Targets

Since our main motivation was the study of miRNAs that regulate the formation and differentiation of the periderm, particularly TDP tissues, we started by analysing the miRNAs uniquely detected in these tissues. By applying an FDR < 0.05 to the sequences expressed in at least two TDP libraries and absent in DX, a total of 261 sequences remained, including 140 novel miRNAs, 78 conserved and 43 tasi-RNAs (Table S4.1). The top 20 most expressed sequences in TDP tissues (Table S4.2) included members of MIR156, MIR165/66, MIR167, MIR397 and MIR479, and several novel miRNAs and tasi-RNAs.

Prediction of targets for these 20 sequences returned over 5000 transcripts (Table S5.1), from which a total of 440 unique target transcripts have been also identified by previous RNA-seq analysis performed to the same TDP tissues (Lopes et al. 2020) (Table S5.2). A gene set enrichment analysis performed on the 440 unique target transcripts revealed 45 enriched GO terms (Table S6.1). Within the biological process (BP) domain, the terms transport, cell communication, protein phosphorylation, ion transport and signalling were the most represented ones, while membrane, plasma membrane and apoplast were the most enriched in the cellular component (CC) domain. As to the molecular function (MF) domain, it included the highest number of enriched terms (23), with binding, small-molecule binding and adenyl ribonucleotide binding being the most represented. Some of the identified targets have been previously associated with phellem tissues, including targets encoding several lipid metabolism and transfer proteins, such as GDSL esterase/lipases and ABC transporter G family members as well as members of the cytochrome P450 family, known to be involved in suberin biosynthesis (Table S6.2). Additionally, several members of transcription factor (TF) gene families previously associated with suberized tissues, such as MYB, WRKY, HD-ZIP III, AUX/IAA and ERF, were identified here. Several targets related to defence mechanisms such as those coding for putative disease-resistance proteins RGA4, RPP13 and RGA3, TMV disease-resistance protein and leaf rust 10 disease-resistance locus receptor-like protein kinase (LRK10L) were also identified (Table S6.2).

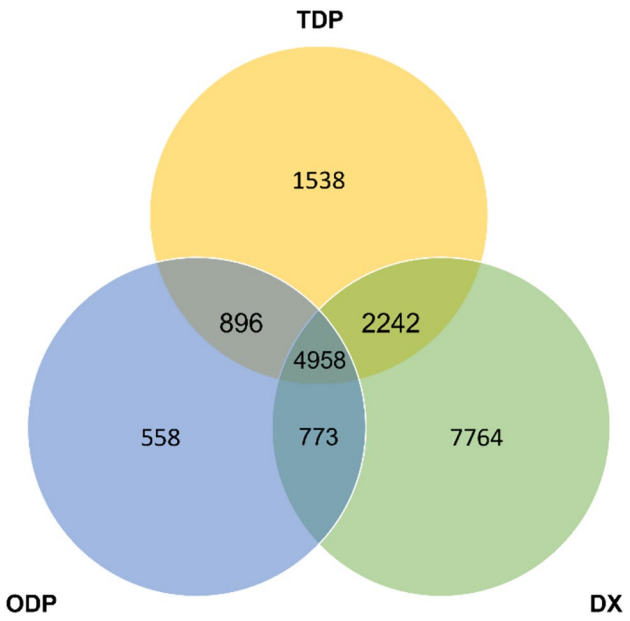

Fig. 1 Venn diagram of differentially expressed small RNAs between traumatic differentiating phellem (TDP), original differentiating phellem (ODP) and differentiating xylem (DX) samples

Differentially Expressed miRNAs in TDP Versus DX

Next, comparative analysis of miRNAs between TDP and DX tissues revealed 246 differentially expressed (DE) miRNAs (74 conserved and 160 novel) and tasi-RNAs (12) (Table S7). From these, 133 are up-regulated in TDP (60 conserved and 63 novel miRNAs), and 113 are up-regulated in xylem (DX), most of which are novel miRNAs (97) (Table S7, Fig. 2). The 74 conserved miRNAs belong to 23 families, with MIR165/166 showing the highest number of isoforms (25), followed by MIR159 (7), and all the other families having between 1 and 4 isoforms (Fig. S2).

Overall, most miRNA families are more expressed in TDP than DX (Fig. 3), except MIR159, MIR169, MIR396 and MIR399 which were predominant in DX. MIR165/166 exhibits the higher expression levels in both tissues, particularly in TDP in which MIR167, MIR168 and MIR390 are also among the more expressed. It should be noted that, in some cases, significant variation occurred across different isoforms within the same miRNA family (Fig. S3). As observed for conserved miRNA families, most novel miRNAs had low to moderate expression levels in both tissues. Nevertheless, a small group of novel miRNAs exhibited higher expression levels, particularly in TDP tissues (Fig. S4).

Fig. 2 Number of conserved miRNAs, novel miRNAs and tasi-RNAs up-regulated in traumatic differentiating phellem (TDP) and differentiating xylem (DX). In both graphs, the numbers correspond to the total sRNAs after the removal of the sequences with expression values equal to zero in at least two libraries of the same tissue and with an FDR < 0.05 and a two-fold-change (FC) cut-off

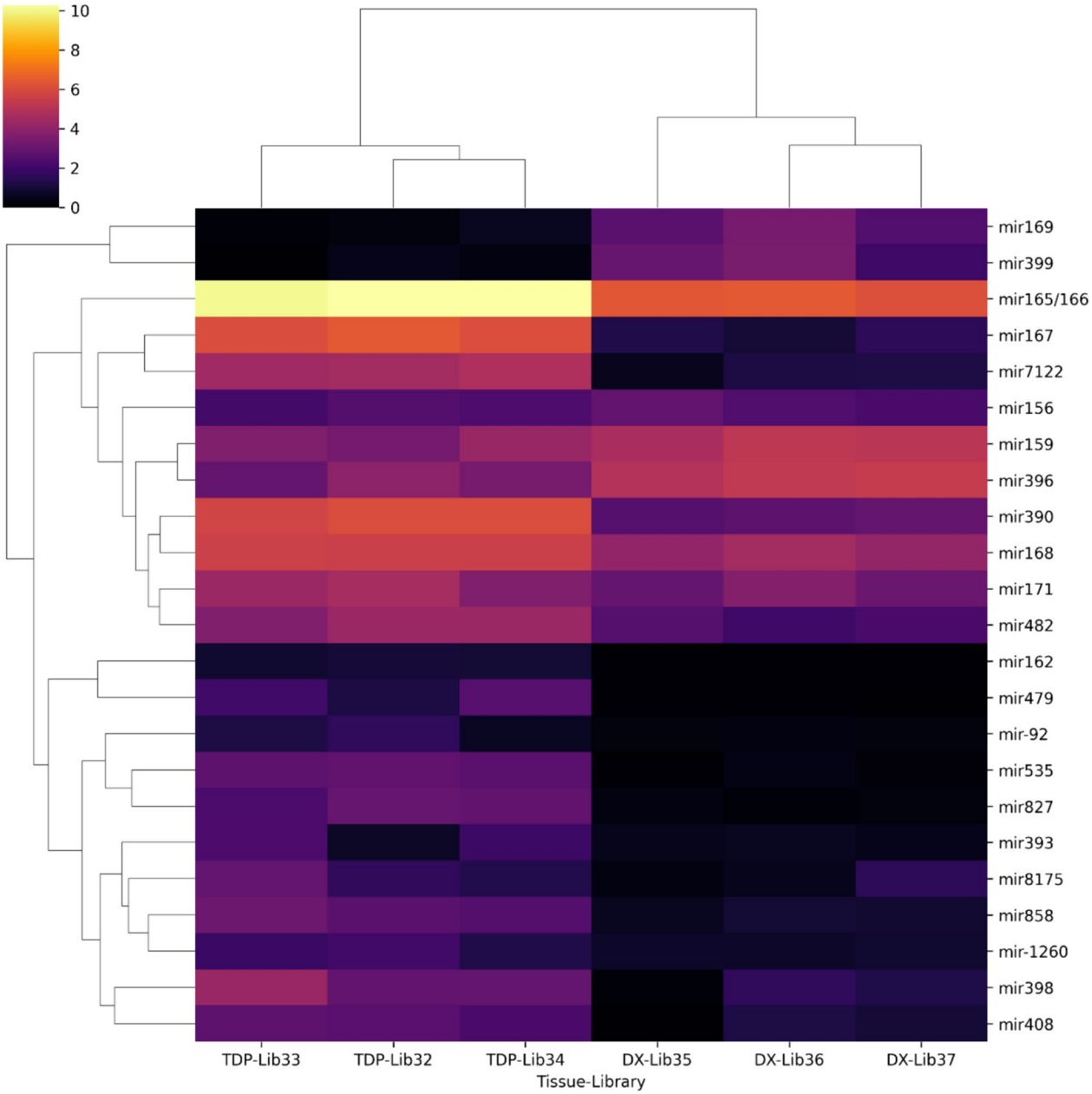

Fig. 3 Expression patterns of conserved miRNA families differentially expressed in traumatic differentiating phellem (TDP) and differentiating xylem (DX). The heatmap was built using CPM (counts per million) expression values

Predicted Targets of miRNAs DE in TDP Versus DX

Over 22,000 target transcripts were predicted for the 246 miRNAs DE between TDP and DX (Table S8.1). By crossing this list with the transcripts identified by RNA-seq of the same samples (Lopes et al. 2020), a total of 17,022 predicted targets were retained (Table S8.2). Furthermore, only 3309 targets with expression values that negatively correlate with the respective miRNA expression (Pearson correlation coefficient below − 0.70) were found, of which 1890 are up-regulated in TDP and 1419 up-regulated in xylem (Table S8.2).

Subsequently, a functional enrichment analysis (p-value < 0.01) of the 3309 predicted targets retrieved 116 over-represented GO terms (Table S9.1). In the CC domain, apart from the endomembrane system, exclusively enriched in DX, all the other terms were enriched in both tissues (Fig. S5a). As for the MF domain, metalloendopeptidase activity, transmembrane receptor protein serine/threonine kinase activity, nucleoside-triphosphatase activity, nucleoside-triphosphatase activity, signalling receptor activity and sequence-specific DNA binding were exclusively enriched in TDP tissues (Fig. S5b). Finally, chloride transport, hormone-mediated signalling pathway, sterol transport and mRNA metabolic process were the most represented BP terms exclusive of TDP tissues (Fig. S5c).

The sequence-specific DNA binding GO term, exclusively enriched in TDP tissues, comprises several TF genes, especially from the MYB family (Table S9.2) and most of them predicted targets of MIR858. Additionally, MIR165/166 is the family with more predicted targets, including HD-ZIP III, WRKY and NAC TFs (Table S9.2). Some potentially interesting TF transcripts targeted by novel miRNAs, such as bHLH36-like, ATHB13-like, WRKY71, WRKY14, MYB20-like and MERISTEM L1-like (Table S9.2), have been also identified in the transcriptomic analysis of coding transcripts (Lopes et al. 2020). The hormone-mediated signalling pathway term, exclusively enriched in TDP tissues, also contains potentially interesting candidates previously identified by Lopes et al. (2020), such as transcripts coding auxin responsive protein IAA11, ARF18 and ARF19, all regulated by novel miRNAs (Table S9.2).

Differential Expression Analysis Between TDP and ODP

The comparison between differentiating phellem from original (ODP) and traumatic phellogen (TDP) ("virgin" vs "amadia" cork) retrieved only 12 DE miRNAs, including 4 conserved miRNAs (miR395_1, miR395_4, miR159_1 and miR398_1) and 8 novel miRNAs (Table S10). A total of 1114 targets were predicted, of which 805 are annotated (Table S11.1). From these, 695 transcripts had been also identified in the previous RNA-seq analysis of TDP and ODP libraries (Lopes et al. 2020). However, only 28 predicted targets had a negatively correlated expression with their targeting miRNA, with the vast majority being up-regulated in TDP, such as transcripts encoding the abscisic acid receptor PYL8, the calmodulin-binding protein 25-like, the zinc finger CCCH domain-containing protein ZFN-like and methyl-CpG-binding domain-containing protein 2-like (Table S11.2).

miRNA Expression Validation by RT-qPCR

Five conserved miRNAs were chosen for validation of their expression profiles using TaqMan® Assays. These miRNAs were selected based on their potentially interesting targets, RNA-seq expression of their targets (Table S12) and divergent expression levels in TDP/DX tissues. The RT-qPCR values (copy number/ng input) obtained for each one of the three biological replicates in both tissues (TDP and DX) are shown (Fig. 4a). All conserved miRNAs analysed showed significant differences in expression levels between the two tissues. Apart from miR399, more expressed in DX tissues, all the other conserved miRNAs showed higher expression levels in TDP tissues. The RT-qPCR results showed a good agreement with expression profiles obtained from small RNA-seq data with logFC levels varying between − 5.360 (up-regulated in TDP) and 4.521 (down-regulated in TDP) (Fig. S4b). These results are supported by a strong linear correlation between the two analyses, with a determination coefficient $R^2 = 0.98$ (Fig. 4c).

Discussion

Compared to other secondary growth tissues, our understanding of miRNA-mediated regulation of phellogen activity and periderm differentiation is very limited (Milhinhos, Lopes, et al. 2020). The growing interest in this subject is due to the remarkable characteristics of the cork tissue, which make it highly valuable for sustainable industrial applications. Cork oak, in particular, has emerged as an excellent model for identifying regulators involved in cork formation given its unique capacity to continuously produce cork throughout its lifespan, providing an excellent system to gain additional insights into the regulation and function of secondary meristems. The recent availability of cork oak draft genome (Ramos et al. 2018) has further facilitated research in this area.

The analysis of the sRNA size profile showed the predominance of the 24 nt size class in DX and TDP tissues, closely followed by 21 nt, while the opposite tendency is observed in ODP tissues. While the 21 nt size class is usually associated with miRNAs involved in post-transcriptional gene silencing, the 24 nt sRNAs mainly comprise heterochromatic

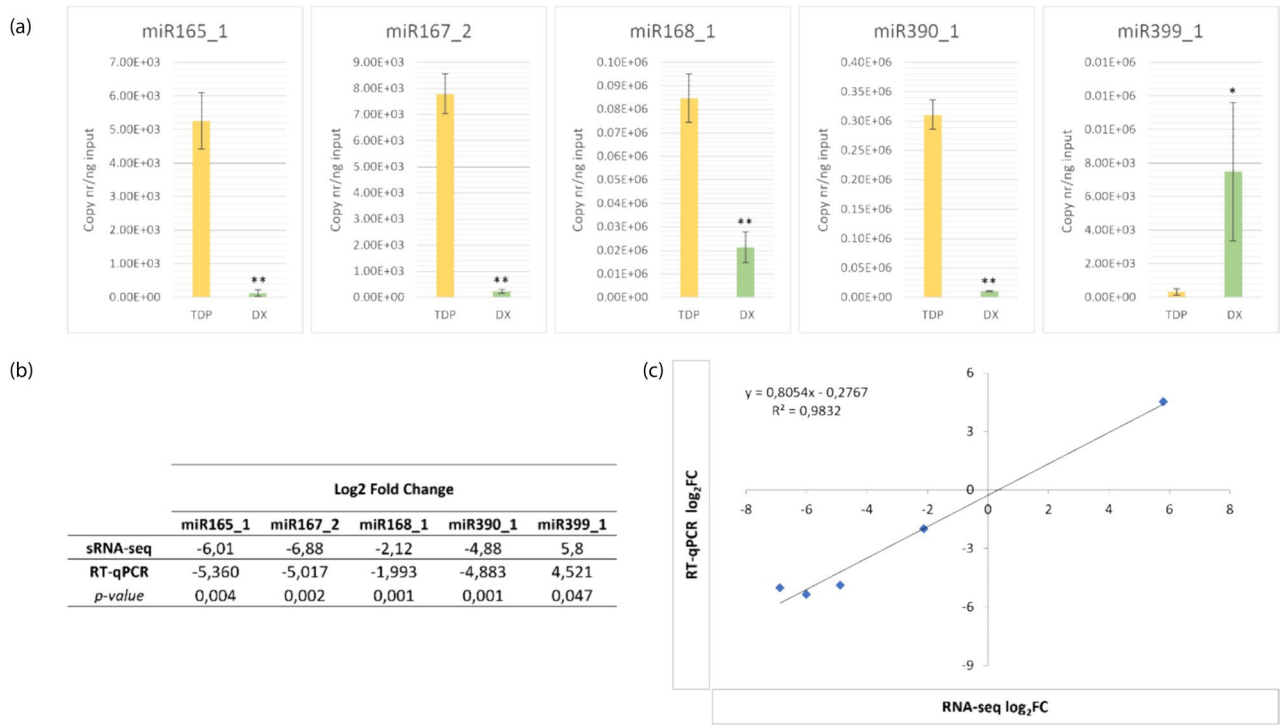

(b)

	Log2 Fold Change				
	miR165_1	miR167_2	miR168_1	miR390_1	miR399_1
sRNA-seq	-6,01	-6,88	-2,12	-4,88	5,8
RT-qPCR	-5,360	-5,017	-1,993	-4,883	4,521
p-value	0,004	0,002	0,001	0,001	0,047

Fig. 4 Expression profile validation through TaqMan miRNA Assays of five conserved miRNAs. **a** RT-qPCR values (copy number/ng input) of three biological replicates for both tissues (TDP and DX). Data represent the mean ± SD of normalised relative expression for three biological replicates. Statistical significance was calculated with Student's *t*-test (*$p < 0.05$; **$p < 0.01$), **b** comparison of the log2 fold-changes (log2FC) obtained by RT-qPCR and small RNA-seq experiments and **c** linear regression with the correlation coefficient (R^2)

siRNAs (hetsiRNAs) associated with DNA methylation in silencing of transposable elements (TE), highly repetitive rDNA regions and other intergenic sequences, contributing to the preservation of genome integrity (Xie et al. 2012; Borges and Martienssen 2015). Our results are consistent with previous reports on *P. trichocarpa* where xylem sRNAs peak at 24 nt (Barakat et al. 2007; Puzey et al. 2012). Additionally, Ding et al. (2014) reported that the 21 nt sRNAs were the most abundant in the cambium during the dormancy period, while in active growth the 24 nt-long sRNAs were predominant, suggesting their involvement in the regulation of cambium activity, including cell division and differentiation (Ding et al. 2014). Although all the samples here analysed were taken during the active growth period, our results suggest that meristematic activity in ODP might be lower than in the other analysed tissues.

Only 12 miRNAs were found DE between the two types of cork tissues (TDP and ODP), which is in agreement with minor changes detected also in the coding transcriptomes of these two tissue samples (Lopes et al. 2020). Among the DE conserved miRNAs, miR159, miR395 and miR398 have been associated to stress responses (Zhu et al. 2011; Matthewman et al. 2012; Li et al. 2017a, b; Millar et al. 2019; Zheng et al. 2020), although their targets may not be conserved among different species. Also, one of the DE novel miRNAs targets a transcript encoding a calmodulin-binding protein that acts as a mediator of responses to environmental cues (Zhang and Lu 2003). Altogether, these results suggest that the two tissue types may slightly differ at the environmental response level. Interestingly, two of the novel miRNAs DE had a methyl-CpG-binding domain-containing protein 2-like transcript as predicted target, generally associated to gene silencing, suggesting its contribution for some level of epigenetic differentiation previously reported between both tissues (Inácio et al. 2017). An abscisic acid (ABA) receptor PYL8 transcript has also been predicted as target of a novel miRNA up-regulated in TDP, which may be related to differential regulation of suberization given the role of ABA in this process (Cottle and Kolattukudy 1982; Barberon et al. 2016). The lack of significant differences both in the coding and small non-coding transcriptome is somehow surprising, especially considering that the samples originate from different trees. Although a major difference between "virgin" and "amadia" cork is related to the structural components of the cork cell walls, Pereira (1988) reported distinct chemical composition of the suberin of both tissues. It is possible that post-translational regulatory mechanisms, instead of transcriptional and miRNA-mediated post-transcriptional regulation, play a major role. This would be consistent with the functional roles of additionally predicted

targets, such as those coding for ubiquitin carboxyl-terminal hydrolase 25 (putatively targeted by miR395) involved in the proteasomal degradation (Zhou et al. 2017) or the probable UDP-N-acetylglucosamine-peptide N-acetylglucosaminyltransferase SEC (putatively targeted by a novel miRNA) involved in the glycosylation of diverse cytoplasmic and nuclear proteins (Zentella et al. 2023).

In the comparison between TDP and DX, numerous DE miRNAs and tasi-RNAs were identified. The majority of conserved miRNAs, particularly MIR165/166, MIR167, MIR168 and MIR390 families, were up-regulated in TDP tissues. The functional enrichment analysis of the targeted transcripts highlighted the sequence-specific DNA binding GO term in TDP. This indicates the significance of transcriptional regulation by TFs during phellogen activity and phellem differentiation. A recent transcriptomic analysis of cork seasonal growth revealed that transcripts associated with DNA binding capacity, mainly TFs, were also enriched at the early stages of cork growth (Fernández-Piñán et al. 2021). This underscores the crucial role of TF-mediated transcriptional regulation in maintaining phellogen cell proliferation.

MiR165/166 is known for its regulation of the HD-ZIP III transcription factor gene family. In Arabidopsis, this family comprises INTERFASCICULAR FIBERLESS/REVOLUTA (IFL/REV), PHABULOSA (PHB)/ATHB14, PHAVOLUTA (PHV)/ATHB9, CORONA/ATHB15 and ATHB8 (McConnell and Barton 1998; Baima et al. 2001; McConnell et al. 2001; Mallory et al. 2004). In our data, except for PHB and PHV cork oak homologs, other members of the HD-ZIP III class were identified as possible targets of miR165/166. Previous studies in Arabidopsis have demonstrated that the miR165/166—HD-ZIPIII module is involved in several growth and developmental processes including xylem differentiation (Du and Wang 2015; Lopes et al. 2020). The expression of HD-ZIP III genes, along with a local maximum of auxin, promotes xylem identity and cellular quiescence of the organiser cells (Smetana et al. 2019). ATHB8 acts as a positive regulator of procambium and cambium development, stimulating xylem differentiation when overexpressed (Baima et al. 1995, 2001). ATHB15 is known to regulate the vasculature in Arabidopsis inflorescence stems (Kim et al. 2005), and its ortholog POPCORONA in *Populus* trees is implicated in secondary growth (Du et al. 2011). REV plays a fundamental role in regulating cambia and secondary vascular tissue development (Robischon et al. 2011). Important roles for miRNA-regulated expression of HD-ZIP III transcripts in periderm development can be hypothesised but further studies are required to elucidate their contribution to this process.

Our analysis has also highlighted other TF families associated with meristematic activity and secondary growth, including MYB, WRKY and NAC. Interestingly, several MYB TFs have been associated with the suberization process (Cohen et al. 2020). For instance, MYB41 activates suberin synthesis and deposition of cell wall suberin-like lamellae in both *Nicotiana benthamiana* and *Arabidopsis thaliana* (Kosma et al. 2014). *QsMYB1* (MYB84) has been previously identified in *Q. suber* cork tissues associated with responses to heat and drought stresses and plant recovery (Almeida et al. 2013), and directly targets genes involved in suberin and lignin pathways (Capote et al. 2018). Furthermore, MYB107 and MYB9 homologues are required for suberin assembly in the Arabidopsis seed coat (Lashbrooke et al. 2016). The majority of these TF are targeted by MIR858 which, when overexpressed, down-regulates expression of several MYB transcripts, resulting in up-regulation of lignin biosynthetic genes and down-regulation of flavonoid biosynthetic genes (Sharma et al. 2016).

Another worth mentioning miRNA exclusively enriched in TDP tissues is miR156, not previously associated with secondary growth. Interestingly, the Arabidopsis miR156 targets SQUAMOSA PROMOTER BINDING PROTEIN-LIKE (SPL) TF contributing to a cooperative regulation of root meristem activity and shoot regeneration (Barrera-Rojas et al. 2020).

In this study, several potentially relevant miRNA targets related to hormone-mediated signalling pathways have been also identified. Phytohormones, particularly auxins, are major regulators of cambial activity during secondary growth (Uggla et al. 1996; Nilsson et al. 2008; Smetana et al. 2019; Milhinhos et al. 2020a, b). Recently, gibberellin-dependent modulation of the positioning of the auxin maximum within the cambium was shown to determine the fate of stem cell derivatives (Mäkilä et al. 2023). Importantly, it has been shown by Xiao et al. (2020) that auxin is required for cork cambium initiation from the pericycle via ARF5/MONOPTEROS, ARF8 and other ARFs. In our study, we have identified novel miRNAs DE in TDP that are predicted to target several auxin signalling candidates previously highlighted by RNA-seq in the same tissues, including IAA11, ARF18 and ARF19 transcripts (Lopes et al. 2020). Among other ARF genes differentially expressed in TDP and DX, ARF18 has been shown to be up-regulated in TDP, suggesting a differential auxin signalling and response in these two tissue types (Lopes et al. 2020). Furthermore, MIR167 and MIR390, previously implicated in the auxin signalling pathway through the regulation of ARF genes (Wu et al. 2006; Marin et al. 2010), are highly expressed in TDP tissues. Two of the targets of miR167 identified are ARF6 and ARF8, previously associated to flower development in several species (Nagpal et al. 2005; Ru et al. 2006; Wu et al. 2006; Liu et al. 2014), while another potential target previously identified is IAR3 (IAA-Ala Resistant3), known to be required for drought tolerance (Kinoshita et al. 2012). MiR390, on the other hand, is implicated in the cleavage of the non-coding

TRANS-ACTING SIRNA3 (TAS3) transcripts, generating tasi-RNAs that regulate ARF genes (Allen et al. 2005; Marin et al. 2010). This miR390-TAS3-ARF pathway targets ARF2/3/4 and is critical for several aspects of plant growth and development, including developmental timing and lateral root initiation (Fahlgren et al. 2006; Marin et al. 2010). Interestingly, it has been shown that the activity of miR167 and miR390 increased significantly during active growth in Poplar' cambium (Ding et al. 2014). Moreover, MIR 390 has also been previously identified as one of the most expressed miRNA families in the phellem tissues of *Q. suber* (Chaves et al. 2014). Our findings provide further support of the potential relevance of such miRNA–mRNA interactions in phellogen activity and/or cork differentiation. Further studies focusing on auxin signalling should be conducted in the future to enlighten differential pathways acting in the vascular and periderm tissues.

Another highly expressed miRNA in TDP tissues, also identified by Chaves et al. (2014), is miR168. This miRNA putatively targets AGO1, which is a key regulator of miRNA biogenesis (Vaucheret et al. 2006). AGO1 is up-regulated in poplar trees' active cambium (Ding et al. 2014), and it has been identified in TPD transcriptomics data as well (Lopes et al. 2020). The high expression of miR168 in TDP tissues during the peak of phellogen activity suggests a potential role in this process.

In this study, we also identified several novel and conserved miRNAs, as miR159, miR479, miR171 and miR482, which target several transcripts encoding lipid metabolism and transfer proteins as GDSL esterase/lipase and ABC transporter G and cytochrome P450 family members, known to be involved in suberin biosynthesis, transport and assembly (Vishwanath et al. 2015).

Overall, this study provides valuable insights into an additional layer of regulation besides transcriptional regulation, which contributes to shaping the transcriptome during differentiation of phellem from the phellogen. The relevance of some of the targets predicted here in the control of phellem differentiation/phellogen activity aligns with previous studies and emphasises the significance of miRNA-mediated regulation in secondary growth. Furthermore, several conserved and novel miRNAs, along with their putative targets, have been discovered as potential candidates for regulating secondary growth.

Unveiling the specific genetic regulators of phellem (cork) and identifying their variants not only contributes to our understanding of fundamental plant biology but it may also provide relevant information to help improve cork quality, such as increasing its thickness (calibre) and reducing porosity which are among the most important features that confer higher value to this 100% natural and recyclable product. Other potential improvement targets include reducing the time before the first cork harvest or the interval between each harvesting. Although *Q. suber* trees are well adapted to its natural environment, novel insights into phellem genetics might also help to devise strategies leading to increased resilience to changing environmental conditions or pathogens, for instance through experimental approaches relying on the identification of patterns of genetic variation in relevant miRNA–target interactions. In any case, further research is necessary to fully understand the functional roles of such interactions.

Supplementary Information The online version contains supplementary material available at https://doi.org/10.1007/s00344-024-11453-1.

Acknowledgements The authors thank Rui Rebelo (Faculdade de Ciências, Universidade de Lisboa) for providing access to Herdade da Ribeira Abaixo (Grândola, Portugal) for sample collection.

Author Contributions This study was conceived and directed by CMM. AC contributed to the sample collection in selected trees at both cork oak woodlands. SL did the experimental work, including methodology implementation, preparation of sRNA for sequencing and gene expression validation by RT-qPCR. BVC and IC performed the bioinformatics analysis. SL and CMM participated in the analysis of results and their biological interpretation. SL and CMM wrote the paper. All authors read and approved the final manuscript.

Funding Open access funding provided by FCT|FCCN (b-on). This work was supported by Fundação para a Ciência e a Tecnologia, I.P. (FCT/MCTES), through the doctoral fellowships PD/BD/114359/2016 to SL and SFRH/BD/143771/2019 to BC, DL 57/2016/CP1351/CT0003 to IC, and grants GREEN-it (UID/Multi/04551/2013), UIDB/04046/2020 (https://doi.org/10.54499/UIDB/04046/2020) and UIDP/04046/2020 (https://doi.org/10.54499/UIDP/04046/2020) Centre grants from FCT, Portugal (to BioISI).

Declarations

Competing interests The authors declare that they have no conflict of interest.

References

Allen E, Xie Z, Gustafson AM, Carrington JC (2005) microRNA-directed phasing during trans-acting siRNA biogenesis in plants. Cell 121:207–221

Almeida T, Pinto G, Correia B, Santos C, Gonçalves S (2013) QsMYB1 expression is modulated in response to heat and drought

stresses and during plant recovery in *Quercus suber*. Plant Physiol Biochem 73:274–281
Arias-Baldrich C, Silva MC, Bergeretti F, Chaves I, Miguel C, Saibo NJM, Sobral D, Faria D, Barros PM (2020) CorkOakDB-the cork oak genome database portal. Database 2020:1–11
Axtell MJ (2013) Classification and comparison of small RNAs from plants. Annu Rev Plant Biol 64:137–159
Baima S, Nobili F, Sessa G, Lucchetti S, Ruberti I, Morelli G (1995) The expression of the Athb-8 homeobox gene is restricted to provascular cells in *Arabidopsis thaliana*. Development 121:4171–4182
Baima S, Possenti M, Matteucci A, Wisman E, Altamura MM, Ruberti I, Morelli G (2001) The Arabidopsis ATHB-8 HD-Zip protein acts as a differentiation-promoting transcription factor of the vascular meristems. Plant Physiol 126:643–655
Barakat A, Wall PK, DiLoreto S, dePamphilis CW, Carlson JE (2007) Conservation and divergence of microRNAs in Populus. BMC Genomics 8:1–16
Barberon M, Vermeer JEM, De Bellis D, Wang P, Naseer S, Andersen TG, Humbel BM, Nawrath C, Takano J, Salt DE, Geldner N (2016) Adaptation of root function by nutrient-induced plasticity of endodermal differentiation. Cell 164:447–459
Barrera-Rojas CH, Rocha GHB, Polverari L, Pinheiro Brito DA, Batista DS, Notini MM, Da Cruz ACF, Morea EGO, Sabatini S, Otoni WC, Nogueira FTS (2020) MiR156-targeted SPL10 controls Arabidopsis root meristem activity and root-derived de novo shoot regeneration via cytokinin responses. J Exp Bot 71:934–950
Borges F, Martienssen RA (2015) The expanding world of small RNAs in plants. Nat Rev Mol Cell Biol 16:727–741
Capote T, Barbosa P, Usié A, Ramos AM, Inácio V, Ordás R, Gonçalves S, Morais-Cecílio L (2018) ChIP-Seq reveals that QsMYB1 directly targets genes involved in lignin and suberin biosynthesis pathways in cork oak (*Quercus suber*). BMC Plant Biol 18:1–19
Chang S, Puryear J, Cairney J (1993) A simple and efficient method for isolating RNA from pine trees. Plant Mol Biol Report 11:113–116
Chang W, Guo Y, Zhang H, Liu X, Guo L (2020) Same actor in different stages: genes in shoot apical meristem maintenance and floral meristem determinacy in Arabidopsis. Front Ecol Evol 8:1–12
Chaves I, Lin YC, Pinto-Ricardo C, Van de Peer Y, Miguel C (2014) miRNA profiling in leaf and cork tissues of *Quercus suber* reveals novel miRNAs and tissue-specific expression patterns. Tree Genet Genomes 10:721–737
Chaves I, Costa BV, Rodrigues AS, Bohn A, Miguel CM (2017) miRPursuit—a pipeline for automated analyses of small RNAs in model and nonmodel plants. FEBS Lett 591:2261–2268
Chen H, Li YH, Wu SH (2007) Bioinformatic prediction and experimental validation of a microRNA-directed tandem trans-acting siRNA cascade in Arabidopsis. PNAS 104:3318–3323
Cohen H, Fedyuk V, Wang C, Wu S, Aharoni A (2020) SUBERMAN regulates developmental suberization of the Arabidopsis root endodermis. Plant J 102:431–447
Cottle W, Kolattukudy PE (1982) Abscisic acid stimulation of suberization: induction of enzymes and deposition of polymeric components and associated waxes in tissue cultures of potato tuber. Plant Physiol 70:775–780
Dai X, Zhuang Z, Zhao PX (2018) psRNATarget: a plant small RNA target analysis server (2017 release). Nucleic Acids Res 46:W49–W54
Dharmawardhana P, Brunner AM, Strauss SH (2010) Genome-wide transcriptome analysis of the transition from primary to secondary stem development in *Populus trichocarpa*. BMC Genomics 11:1–19
Ding Q, Zeng J, He XQ (2014) Deep sequencing on a genome-wide scale reveals diverse stage-specific microRNAs in cambium during dormancy-release induced by chilling in poplar. BMC Plant Biol 14:1–16
Du Q, Wang H (2015) The role of HD-ZIP III transcription factors and miR165/166 in vascular development and secondary cell wall formation. Plant Signal Behav 10:e1078955
Du J, Miura E, Robischon M, Martinez C, Groover A (2011) The Populus class III HD ZIP transcription factor POPCORONA affects cell differentiation during secondary growth of woody stems. PLoS ONE 6:e17458
Emery JF, Floyd SK, Alvarez J, Eshed Y, Hawker NP, Izhaki A, Baum SF, Bowman JL (2003) Radial patterning of Arabidopsis shoots by class III HD-ZIP and KANADI genes. Curr Biol 13:1768–1774
Fahlgren N, Montgomery TA, Howell MD, Allen E, Dvorak SK, Alexander AL, Carrington JC (2006) Regulation of AUXIN RESPONSE FACTOR3 by TAS3 ta-siRNA affects developmental timing and patterning in Arabidopsis. Curr Biol 16:939–944
Fernández-Piñán S, Boher P, Soler M, Figueras M, Serra O (2021) Transcriptomic analysis of cork during seasonal growth highlights regulatory and developmental processes from phellogen to phellem formation. Sci Rep 11:1–14
Graça J, Pereira H (2004) The periderm development in *Quercus suber*. IAWA J 25:325–335
Ilegems M, Douet V, Meylan-Bettex M, Uyttewaal M, Brand L, Bowman JL, Stieger PA (2010) Interplay of auxin, KANADI and Class III HD-ZIP transcription factors in vascular tissue formation. Development 137:975–984
Inácio V, Barros PM, Costa A, Roussado C, Gonçalves E, Costa R, Graça J, Oliveira MM, Morais-Cecílio L (2017) Differential DNA methylation patterns are related to phellogen origin and quality of *Quercus suber* cork. PLoS ONE 12:e0169018
Jones-Rhoades MW (2012) Conservation and divergence in plant microRNAs. Plant Mol Biol 80:3–16
Kim J, Jung J, Reyes JL, Kim Y, Kim S, Chung K, Kim JA, Lee M, Lee Y, Kim VN, Chua N, Park C (2005) microRNA-directed cleavage of ATHB15 mRNA regulates vascular development in Arabidopsis inflorescence stems. Plant J 42:84–94
Kinoshita N, Wang H, Kasahara H, Liu J, MacPherson C, Machida Y, Kamiya Y, Hannah MA, Chua NH (2012) IAA-Ala Resistant3, an evolutionarily conserved target of miR167, mediates Arabidopsis root architecture changes during high osmotic stress. Plant Cell 24:3590–3602
Knauer S, Holt AL, Rubio-Somoza I, Tucker EJ, Hinze A, Pisch M, Javelle M, Timmermans MC, Tucker MR, Laux T (2013) A protodermal miR394 signal defines a region of stem cell competence in the Arabidopsis shoot meristem. Dev Cell 24:125–132
Ko JH, Prassinos C, Han KH (2006) Developmental and seasonal expression of PtaHB1, a Populus gene encoding a class III HD-Zip protein, is closely associated with secondary growth and inversely correlated with the level of microRNA (miR166). New Phytol 169:469–478
Kosma DK, Murmu J, Razeq FM, Santos P, Bourgault R, Molina I, Rowland O (2014) AtMYB41 activates ectopic suberin synthesis and assembly in multiple plant species and cell types. Plant J 80:216–229
Kozomara A, Griffiths-Jones S (2014) miRBase: annotating high confidence microRNAs using deep sequencing data. Nucleic Acids Res 42:D68–D73
Lashbrooke J, Cohen H, Levy-Samocha D, Tzfadia O, Panizel I, Zeisler V, Massalha H, Stern A, Trainotti L, Schreiber L, Costa F, Aharoni A (2016) MYB107 and MYB9 homologs regulate suberin deposition in angiosperms. Plant Cell 28:2097–2116
Laufs P, Peaucelle A, Morin H, Traas J (2004) MicroRNA regulation of the CUC genes is required for boundary size control in *Arabidopsis meristems*. Development 131:4311–4322

Li S, Castillo-González C, Yu B, Zhang X (2017a) The functions of plant small RNAs in development and in stress responses. Plant J 90:654–670

Li L, Yi H, Xue M, Yi M (2017b) miR398 and miR395 are involved in response to SO2 stress in *Arabidopsis thaliana*. Ecotoxicology 26:1181–1187

Liu N, Wu S, Van HJ, Wang Y, Ding B, Fei Z, Clarke TH, Reed JW, Van Der Knaap E (2014) Down-regulation of AUXIN RESPONSE FACTORS 6 and 8 by microRNA 167 leads to floral development defects and female sterility in tomato. J Exp Bot 65:2507–2520

Liu C, Ma D, Wang Z, Chen N, Ma X, He XQ (2022) MiR395c regulates secondary xylem development through sulfate metabolism in poplar. Front Plant Sci 13:1756

Lopes ST, Sobral D, Costa B, Perdiguero P, Chaves I, Costa A, Miguel CM (2020) Phellem versus xylem: genome-wide transcriptomic analysis reveals novel regulators of cork formation in cork oak. Tree Physiol 40:129–141

Mäkilä R, Wybouw B, Smetana O, Vainio L, Solé-Gil A, Lyu M, Ye L, Wang X, Siligato R, Jenness MK, Murphy AS, Mähönen AP (2023) Gibberellins promote polar auxin transport to regulate stem cell fate decisions in cambium. Nat Plants 9:631–644

Mallory AC, Reinhart BJ, Jones-Rhoades MW, Tang G, Zamore PD, Barton KM, Bartel DP (2004) MicroRNA control of PHABULOSA in leaf development: importance of pairing to the microRNA 5' region. EMBO J 23:3356–3364

Marin E, Jouannet V, Herz A, Lokerse AS, Weijers D, Vaucheret H, Nussaume L, Crespi MD, Maizel A (2010) mir390, Arabidopsis TAS3 tasiRNAs, and their AUXIN RESPONSE FACTOR targets define an autoregulatory network quantitatively regulating lateral root growth. Plant Cell 22:1104–1117

Matthewman CA, Kawashima CG, Húska D, Csorba T, Dalmay T, Kopriva S (2012) miR395 is a general component of the sulfate assimilation regulatory network in Arabidopsis. FEBS Lett 586:3242–3248

McConnell JR, Barton MK (1998) Leaf polarity and meristem formation in Arabidopsis. Development 125:2935–2942

McConnell JR, Emery J, Eshed Y, Bao N, Bowman J, Barton MK (2001) Role of PHABULOSA and PHAVOLUTA in determining radial patterning in shoots. Nature 411:709–713

Milhinhos A, Bollhöner B, Blazquez MA, Novák O, Miguel CM, Tuominen H (2020a) ACAULIS5 is required for cytokinin accumulation and function during secondary growth of Populus trees. Front Plant Sci 11:601858

Milhinhos A, Lopes S, Miguel C (2020b) microRNA-mediated regulation of plant vascular development and secondary growth. In: Miguel C, Dalmay T, Chaves I (eds) Plant microRNAs—shaping development and environmental responses. Springer, Cham, pp 143–168

Millar AA, Lohe A, Wong G (2019) Biology and function of miR159 in plants. Plants 8:255

Moxon S, Schwach F, Dalmay T, Maclean D, Studholme DJ, Moulton V (2008) A toolkit for analysing large-scale plant small RNA datasets. Bioinformatics 24:2252–2253

Nagpal P, Ellis CM, Weber H, Ploense SE, Barkawi LS, Guilfoyle TJ, Hagen G, Alonso JM, Cohen JD, Farmer EE, Ecker JR, Reed JW (2005) Auxin response factors ARF6 and ARF8 promote jasmonic acid production and flower maturation. Development 132:4107–4118

Natividade J (1950) Subericultura. Ministério da Agric Pescas e Aliment Direcção-Geral das Florestas

Nilsson J, Karlberg A, Antti H, Lopez-Vernaza M, Mellerowicz E, Perrot-Rechenmann C, Sandberg G, Bhalerao RP (2008) Dissecting the molecular basis of the regulation of wood formation by auxin in hybrid aspen. Plant Cell 20:843–855

Pereira H (1988) Chemical composition and variability of cork from *Quercus suber* L. Wood Sci Technol 22:211–218

Pereira H (2007) The chemical composition of cork. Cork 8:55–99

Puzey JR, Karger A, Axtell M, Kramer EM (2012) Deep annotation of *Populus trichocarpa* microRNAs from diverse tissue sets. PLoS ONE 7:e33034

Qin Z, Li C, Mao L, Wu L (2014) Novel insights from non-conserved microRNAs in plants. Front Plant Sci 5:1–10

Ragni L, Greb T (2018) Secondary growth as a determinant of plant shape and form. Semin Cell Dev Biol 79:58–67

Ramos AM, Usié A, Barbosa P, Barros PM, Capote T, Chaves I, Simões F, Abreu I, Carrasquinho I, Faro C, Guimarães JB, Mendonça D, Nóbrega F, Rodrigues L, Saibo NJM, Varela MC, Egas C, Matos J, Miguel CM, Oliveira MM, Ricardo CP, Gonçalves S (2018) The draft genome sequence of cork oak. Sci Data 5:1–12

Robinson MD, McCarthy DJ, Smyth GK (2009) edgeR: a bioconductor package for differential expression analysis of digital gene expression data. Bioinformatics 26:139–140

Robischon M, Du J, Miura E, Groover A (2011) The Populus Class III HD ZIP, popREVOLUTA, influences cambium initiation and patterning of woody stems. Plant Physiol 155:1214–1225

Ru P, Xu L, Ma H, Huang H (2006) Plant fertility defects induced by the enhanced expression of microRNA167. Cell Res 16:457–465

Sharma D, Tiwari M, Pandey A, Bhatia C, Sharma A, Trivedi PK (2016) MicroRNA858 ss a potential regulator of phenylpropanoid pathway and plant development. Plant Physiol 171:944–959

Smetana O, Mäkilä R, Lyu M, Amiryousefi A, Sánchez Rodríguez F, Wu MF, Solé-Gil A, Leal Gavarrón M, Siligato R, Miyashima S, Roszak P, Blomster T, Reed JW, Broholm S, Mähönen AP (2019) High levels of auxin signalling define the stem-cell organizer of the vascular cambium. Nature 565:485–489

Soler M, Serra O, Molinas M, García-Berthou E, Caritat A, Figueras M (2008) Seasonal variation in transcript abundance in cork tissue analyzed by real time RT-PCR. Tree Physiol 28:743–751

Stocks MB, Moxon S, Mapleson D, Woolfenden HC, Mohorianu I, Folkes L, Schwach F, Dalmay T, Moulton V (2012) The UEA sRNA workbench: a suite of tools for analysing and visualizing next generation sequencing microRNA and small RNA datasets. Bioinformatics 28:2059–2061

Tang F, Wei H, Zhao S, Wang L, Zheng H, Lu M (2016) Identification of microRNAs involved in regeneration of the secondary vascular system in *Populus tomentosa* carr. Front Plant Sci 7:1–17

Uggla C, Moritz T, Sandberg G, Sundberg B (1996) Auxin as a positional signal in pattern formation in plants. Proc Natl Acad Sci 93:9282–9286

Vaucheret H, Mallory AC, Bartel DP (2006) AGO1 homeostasis entails coexpression of MIR168 and AGO1 and preferential stabilization of miR168 by AGO1. Mol Cell 22:129–136

Vishwanath SJ, Delude C, Domergue F, Rowland O (2015) Suberin: biosynthesis, regulation, and polymer assembly of a protective extracellular barrier. Plant Cell Rep 34:573–586

Wang J, Bao J, Zhou B, Li M, Li X, Jin J (2021) The osa-miR164 target OsCUC1 functions redundantly with OsCUC3 in controlling rice meristem/organ boundary specification. New Phytol 229:1566–1581

Wang L, Hou J, Xu H, Zhang Y, Huang R, Wang D, He XQ (2022) The PtoTCP20-miR396d-PtoGRF15 module regulates secondary vascular development in Populus. Plant Commun 4:100494

Williams L, Grigg SP, Xie M, Christensen S, Fletcher JC (2005) Regulation of Arabidopsis shoot apical meristem and lateral organ formation by microRNA miR166g and its AtHD-ZIP target genes. Development 132:3657–3668

Wu M, Tian Q, Reed JW (2006) Arabidopsis microRNA167 controls patterns of ARF6 and ARF8 expression, and regulates both female and male reproduction. Development 133:4211–4218

Xiao W, Molina D, Wunderling A, Ripper D, Vermeer JEM, Ragni L (2020) Pluripotent pericycle cells trigger different growth outputs

by integrating developmental cues into distinct regulatory modules. Curr Biol 30:4384–4398
Xie Z, Jia G, Ghosh A (2012) Small RNAs in plants. In: Sunkar R (ed) MicroRNAs in plant development and stress responses. Springer, Cham, pp 1–28
Zentella R, Wang Y, Zahn E, Hu J, Jiang L, Shabanowitz J, Hunt DF, Sun T (2023) SPINDLY O-fucosylates nuclear and cytoplasmic proteins involved in diverse cellular processes in plants. Plant Physiol 191:1546–1560
Zhang L, Lu YT (2003) Calmodulin-binding protein kinases in plants. Trends Plant Sci 8:123–127
Zhang Z, Zhang X (2012) Argonautes compete for miR165/166 to regulate shoot apical meristem development. Curr Opin Plant Biol 15:652–658
Zheng Z, Wang N, Jalajakumari M, Blackman L, Shen E, Verma S, Wang M-B, Millar AA (2020) miR159 represses a constitutive pathogen defense. Plant Physiol 182:2182–2198
Zhou G, Kubo M, Zhong R, Demura T (2007) Overexpression of miR165 affects apical meristem formation, organ polarity establishment and vascular development in Arabidopsis. Plant Cell Physiol 48:391–404
Zhou H, Zhao J, Cai J, Patil SB (2017) UBIQUITIN-SPECIFIC PROTEASES function in plant development and stress responses. Plant Mol Biol 94:565–576
Zhu C, Ding Y, Liu H (2011) MiR398 and plant stress responses. Physiol Plant 143:1–9